

## 难变形材料复杂构件精确塑性成形专题

# 轻量化拼焊板构件塑性成形研究进展

詹梅<sup>1a,1b,1c</sup>, 邢路<sup>1a,1b,1c</sup>, 高鹏飞<sup>1a,1b,1c</sup>, 马鹏宇<sup>1a,1b,1c</sup>, 马飞<sup>2</sup>

(1. 西北工业大学 a. 陕西省高性能精确成形技术与装备重点实验室;  
b. 凝固技术国家重点实验室; c. 材料学院, 西安 710072;  
2. 中国航天科技集团公司长征机械厂, 成都 610100)

**摘要:** 拼焊板构件因容易实现轻量化、低成本、短周期成形制造而被广泛应用于飞机、汽车工业中, 但在这类构件的塑性成形中, 焊缝引入的材料、几何、边界条件非线性显著增加了成形复杂性, 导致成形质量及成形极限下降, 尤其是在具有强烈不均匀变形特征的弯曲、旋压等局部加载塑性成形中表现得更加明显, 极大制约了轻量化拼焊板构件的精确塑性成形。为此, 国内外学者在拼焊板构件弯曲及旋压变形机理与成形规律方面开展了大量研究。从焊接材料不均匀力学行为表征、拼焊板构件弯曲及旋压成形有限元建模、焊缝特征对变形行为影响及工艺设计等方面综述了相关研究进展, 最后提出了拼焊板构件塑性成形仍面临的关键难题与挑战, 对认识和发展轻量化拼焊板构件塑性成形具有重要指导意义和参考价值。

**关键词:** 轻量化拼焊板构件; 不均匀力学行为表征; 弯曲成形; 旋压成形; 研究进展

**DOI:** 10.3969/j.issn.1674-6457.2019.05.001

中图分类号 : TG301; TG306 文献标识码 : A 文章编号 : 1674-6457(2019)05-0001-12

## Advances in Plastic Forming of Light-weight Components with Tailor Welded Plate

ZHAN Mei<sup>1a,1b,1c</sup>, XING Lu<sup>1a,1b,1c</sup>, GAO Peng-fei<sup>1a,1b,1c</sup>, MA Peng-yu<sup>1a,1b,1c</sup>, MA Fei<sup>2</sup>

(1. a. Shaanxi Key Laboratory of High-Performance Precision Forming Technology and Equipment; b. State Key Laboratory of Solidification Processing; c. School of Materials Science and Engineering, Northwestern Polytechnical University, Xi'an 710072, China;  
2. Changzheng Machinery Factory, China Aerospace Science and Technology Corporation, Chengdu 610100, China)

**ABSTRACT:** Components with tailor welded plate have gained increasing application in the aircraft and automotive industries because of their advantages: easily achieving forming at light-weight, low cost and short cycle of forming and manufacturing. However, non-linearities of the material, geometry, boundary conditions introduced by the weld increase the forming complexity and deformation unevenness, resulting in a decrease in the forming quality and limit. Especially in the local loading plastic forming with strong uneven deformation characteristics such as bending and spinning, the influences are more obvious. Huge efforts have been made by schoolers at home and abroad to investigate the deformation mechanism and forming law of components with tailor welded plate in the bending and spinning. This paper reviewed the research progress in the characterization of non-uniform mechanical behavior of welded materials, the finite element modeling, the influence of the weld characteristics on the deformation behavior and the process design in the bending and spinning of the tailor welded plate. Finally, the key problems and challenges in the current plastic forming of tailor welded plate were proposed. It provides a fundamental guidance for plastic forming of light-weight components with tailor welded plate.

**KEY WORDS:** components with tailor welded plate; characterization of non-uniform mechanical behavior; bending; spinning; research progress

收稿日期: 2019-07-02

基金项目: 国家杰出青年科学基金 (51625505); 航天先进制造技术联合基金 (U1537203)

作者简介: 詹梅 (1972—), 女, 博士, 教育部“长江学者”特聘教授, 中组部“万人计划”领军人才, 主要研究方向为高性能构件精确塑性成形理论与技术。

随着环境保护、可持续发展和节约型政策的实施,各种拼焊板构件因容易实现轻量化、低成本、短周期的成形制造而在飞机、汽车工业中获得日益广泛的应用<sup>[1—4]</sup>。在这类构件的塑性成形过程中,焊缝、热影响区(Heat affected zone,简称HAZ)和母材组织与性能的不均匀带来了复杂的材料非线性;焊缝、热影响区宽度及其在成形过程中的位置变化带来了复杂的几何非线性;另外,拼焊板与工模具间存在更为复杂的接触与边界条件非线性。这些因素使其不同于均质材料塑性成形,加剧了变形不均匀性及产生缺陷的可能性,制约了此类构件的精确成形制造,因此有必要开展拼焊板构件塑性成形理论及技术研究,以提高成形质量及成形极限。

目前,轻量化拼焊板构件的塑性成形主要包括内高压成形、冲压成形、弯曲成形及旋压成形<sup>[5]</sup>。内高压成形方面,文献[6—10]研究了焊管内高压成形变形特征,获得了成形过程中构件应力应变分布、壁厚变化、开裂规律、焊缝移动规律等,揭示了焊缝性能、位置对内高压成形规律、成形性能及成形极限的影响;冲压成形方面,文献[11—18]研究了焊缝不均匀移动规律及其影响因素,提出了焊缝移动控制方法,提高了拼焊板冲压成形性能。相比于内高压成形及冲压成形,弯曲成形及旋压成形均属于多模具多因素耦合作用下的复杂局部加载塑性成形过程,本身具有强烈的不均匀变形特征,而焊缝带来的材料非线性、几何非线性及边界条件非线性,进一步加剧了变形不均匀性,更容易产生失稳起皱、破裂、截面畸变、凸缘摆动等缺陷,严重制约了拼焊板构件弯曲成形及旋压成形的发展。如何准确表征拼焊板不均匀力学行为、揭示焊缝对拼焊板

弯曲和旋压成形不均匀变形行为作用机理,是提升拼焊板构件弯曲与旋压成形面临的两个关键问题。

西北工业大学詹梅教授团队针对以上两个关键问题,重点在焊接材料不均匀力学行为表征、焊管数控弯曲和拼焊板旋压有限元建模、焊缝特征对弯曲变形行为影响及拼焊板旋压工艺设计方面开展了系统研究,并取得重要进展。文中将重点综述上述研究进展,并指出了轻量化拼焊板构件塑性成形中仍需研究解决的问题。

## 1 焊接接头不均匀力学行为表征

焊接过程中,材料经历热循环作用,且不同区域的温度历史不同,导致各区域间组织及性能存在差异,且各区域内部温度连续变化,因此区域内所形成的组织及性能具有一定连续不均匀性<sup>[19—21]</sup>。准确描述焊接接头不均匀力学行为是精确预测拼焊板构件变形行为的关键前提。

Cheng 等<sup>[22]</sup>、Lee 等<sup>[23]</sup>、Reis 等<sup>[24]</sup>和 Li 等<sup>[25]</sup>分别采用微小拉伸实验、混合材料单向拉伸实验,结合等应变混合法则、显微硬度经验公式、三维数字图像技术确定了焊缝与热影响区的均质本构模型。Song 等<sup>[26]</sup>和 Zhan 等<sup>[27]</sup>在此基础上,分别利用纳米压痕实验和显微硬度实验表征了热影响区内材料属性非均质特征,建立了焊缝+细分热影响区本构模型,这类本构模型虽然考虑了热影响区内材料属性的不均匀性,但忽略了其连续变化特征。为此, Xing 等<sup>[28]</sup>采用图 1 所示的流程,利用纯母材试样和混合材料试样单向拉伸试验(见图 2),结合接头显微硬度连续分

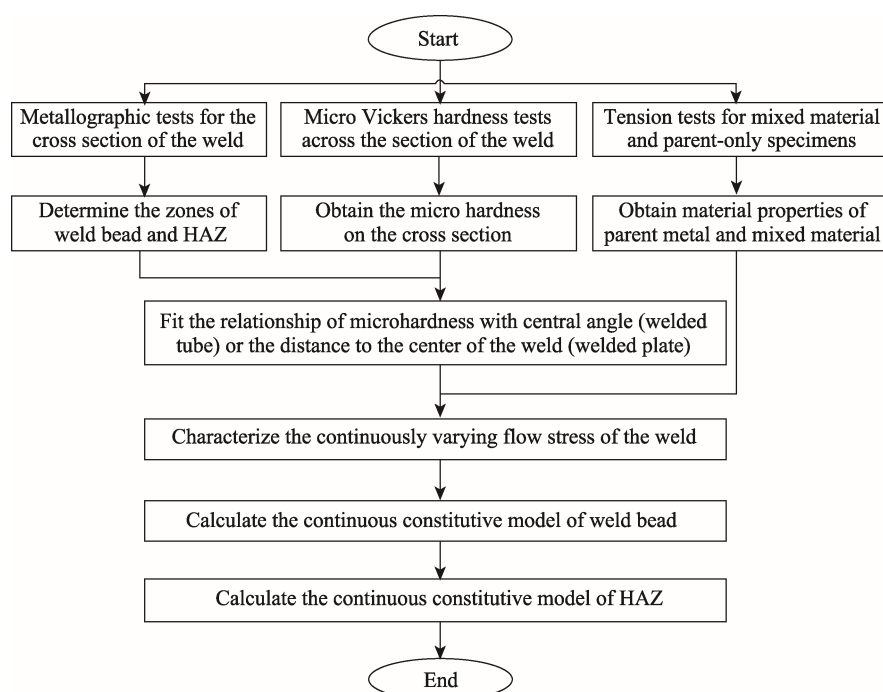


图 1 焊接材料连续本构模型建立流程<sup>[28]</sup>  
Fig.1 Flow chart of developing the continuous constitutive model of welded metal

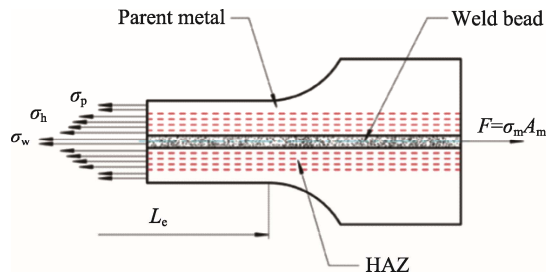


图 2 接头混合材料试样拉伸示意图<sup>[28]</sup>  
Fig.2 Schematic diagram of tension of the mixed material specimen

布(见式(1)),并基于等应变混合法则(见式(2)),建立了考虑焊缝、热影响区和母材性能连续变化的非均质材料本构(见式(3))。

$$\begin{cases} h_{hr} = h_w - (h_w - h_p)(1 - e^{-\xi_1 \alpha}) & \alpha_{wr} \leq \alpha \leq \alpha_{hr} \\ h_{hl} = h_w - (h_w - h_p)(1 - e^{-\xi_2 \alpha}) & \alpha_{hl} \leq \alpha \leq \alpha_{wl} \end{cases} \quad (1)$$

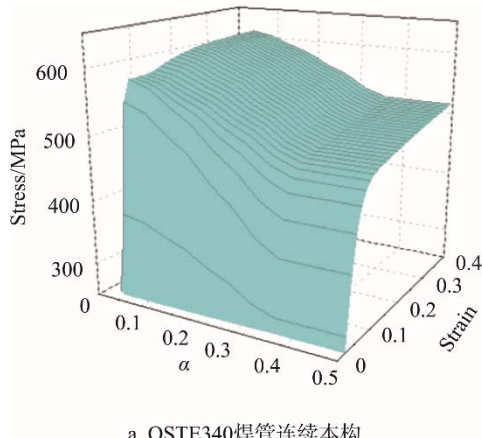
式中:  $\alpha_{wr}$ ,  $\alpha_{wl}$ ,  $\alpha_{hr}$ ,  $\alpha_{hl}$  分别代表焊管内焊缝、热

$$\begin{cases} \sigma_w = \frac{\sigma_m(\alpha_{mr} - \alpha_{ml}) - \sigma_p(\alpha_{mr} + \alpha_{wl} - \alpha_{ml} - \alpha_{wr} + M_1 + M_2)}{\alpha_{wr} - \alpha_{wl} - M_1 - M_2} \\ \sigma_{hr} = \sigma_w - (\sigma_w - \sigma_p)(1 - e^{-\xi_1 \alpha}) \\ \sigma_{hl} = \sigma_w - (\sigma_w - \sigma_p)(1 - e^{-\xi_2 \alpha}) \end{cases}$$

式中:  $\sigma_w$ ,  $\sigma_{hr}$ ,  $\sigma_{hl}$  分别是焊缝内、焊缝右侧热影响区、焊缝左侧热影响区内的流动应力;  $\xi_1$  和  $\xi_2$  均是系数; 参数  $M_1$  和  $M_2$  可根据式(4)确定。

$$\begin{cases} M_1 = \frac{1}{\xi_1}(e^{-\xi_1 \alpha_{hr}} - e^{-\xi_1 \alpha_{wr}}) \\ M_2 = \frac{1}{\xi_2}(e^{-\xi_2 \alpha_{wl}} - e^{-\xi_2 \alpha_{hl}}) \end{cases} \quad (4)$$

将上述方法应用于焊管及拼焊板接头本构模型的建立,确定了QSTE340焊管连续本构及2219铝合金拼焊板连续本构模型,分别如图4a和4b所示。通过对比焊接接头纵向拉伸载荷位移及横向拉伸应变分布的模拟与实验结果(见图5),验证了利用上述方法所得本构模型对准确预测焊接接头变形行为的有效性。



a QSTE340焊管连续本构

影响区、母材界面处的中心角,如图3中标注。

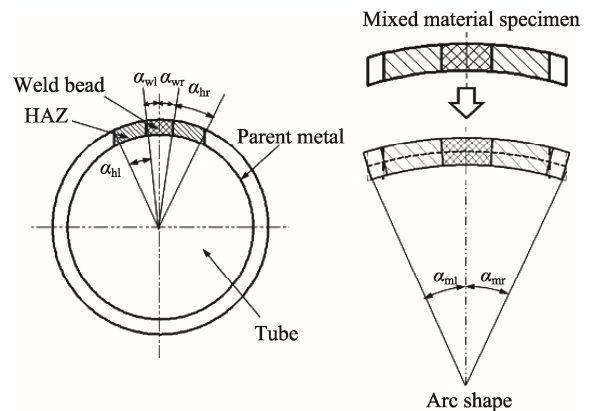


图 3 焊管和混合材料试样截面<sup>[28]</sup>  
Fig.3 Cross sections of welded tube and mixed material specimen

$$\sigma_w A_w + \sigma_h A_h + \sigma_p A_p = \sigma_m A_m \quad (2)$$

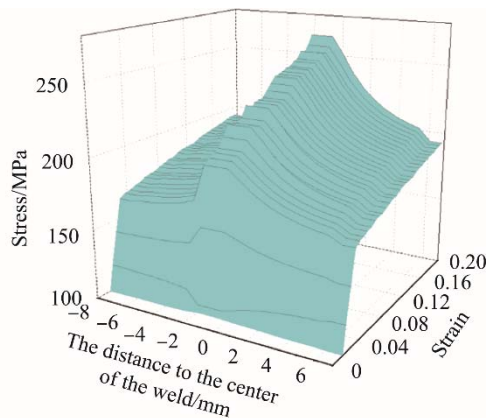
$$\alpha_{wl} \leq \alpha \leq \alpha_{wr}$$

$$\alpha_{wr} \leq \alpha \leq \alpha_{hr}$$

$$\alpha_{hl} \leq \alpha \leq \alpha_{wl}$$

## 2 焊管数控弯曲成形

管材数控弯曲成形过程复杂,影响因素众多,导致弯曲成形过程精确控制较为困难,同时焊管内材料属性不均匀且焊缝位置多变,导致焊管弯曲成形分析更为复杂。西北工业大学任宁等<sup>[29-35]</sup>基于动态显式有限元法,建立了焊管数控弯曲有限元模型(见图6);采用静态隐式有限元法,建立了焊管数控弯曲卸载回弹有限元模型。通过分析模拟与实验相同条件下管材外侧脊线壁厚变化、截面扁化程度,验证了弯曲模型的正确性(见图7),通过对回弹角结果,验证了回弹模型的可靠性(见图8)。



b 2219铝合金拼焊板连续本构<sup>[28]</sup>

图 4 Xing 等<sup>[28]</sup>建立的焊接接头连续本构  
Fig.4 Continuous constitutive model of welded joint established by Xing, et al

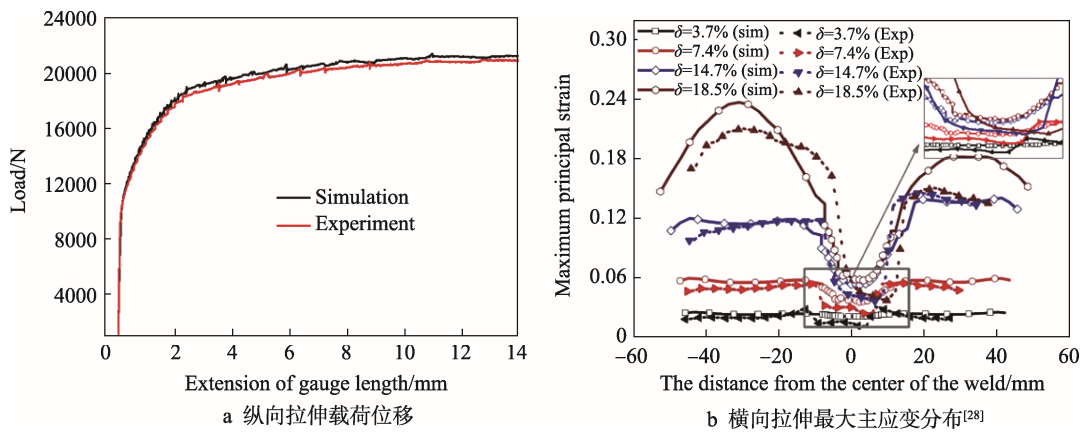


图 5 焊接接头单向拉伸实验与模拟结果对比  
Fig.5 Comparisons between simulation and experiment

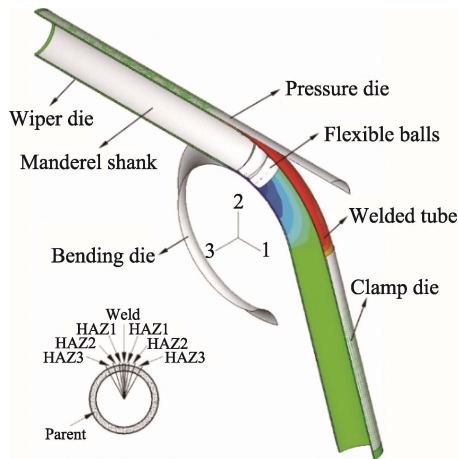


图 6 QSTE340 焊管数控弯曲有限元模型<sup>[33]</sup>  
Fig.6 Finite element model for numerical control bending of QSTE340 welded tube

焊管数控弯曲与均质管数控弯曲相比，焊缝的存在会对成形过程产生较大影响，为此分析焊缝特征（包括位置、宽度、形状系数）对管弯曲变形行为、成形质量、变形协调规律及回弹预测的影响至关重要。西北工业大学詹梅教授团队在该方面做了大量研究<sup>[33]</sup>，具体结果如下。

## 2.1 焊管数控弯曲应力应变分布及成形质量

图 9 所示为弯曲角度 90°、弯曲半径 90 mm 条件下弯曲结束时不同焊缝位置下的等效应力分布。可以看出，不同焊缝位置下，焊管等效应力分布规律一致，都是外侧呈拉应力，且拉应力数值较大，由外侧向内侧，拉应力数值逐渐减小。对比 3 种焊缝位置下等效应力峰值发现，焊缝位于外侧时的最大，位于内侧的次之，位于中性层的最小。

图 10 所示为不同焊缝位置时焊管等效应变分布，可以看出焊管弯曲过程中，应变集中在弯曲部分，在弯曲部分的外侧主要产生拉应变，从外侧脊线到内侧，拉应变数值逐渐减小。对比 3 种焊缝位置下的等效应变峰值得出：焊缝位于弯曲外侧时，等效应变峰值最

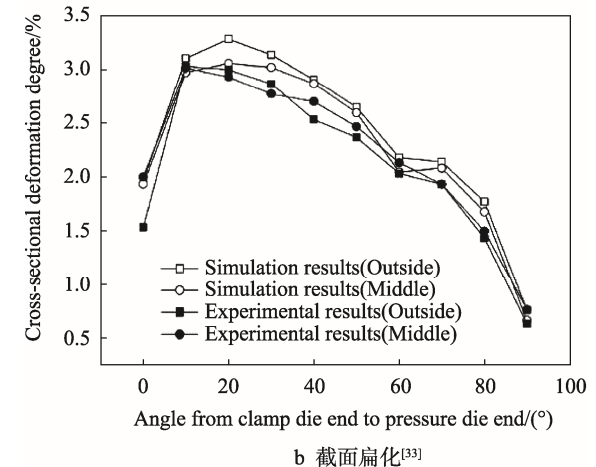
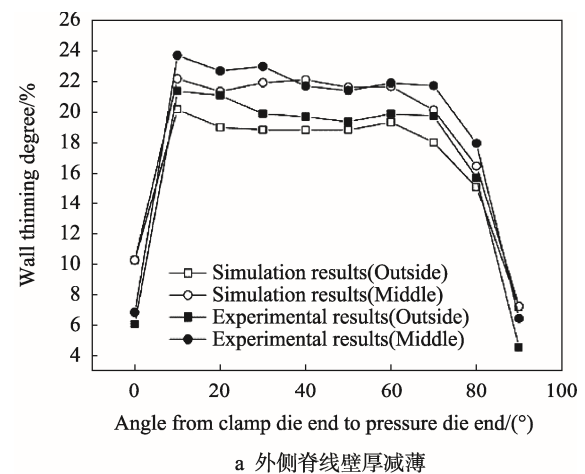


图 7 QSTE340 焊管数控弯曲模拟和实验对比  
Fig.7 Comparisons between simulation and experiment in QSTE340 welded tube bending

大，位于内侧时次之，位于中性层时最小。

不同焊缝位置时，沿焊管弯曲平面中间截面的切向应变、周向应变和厚向应变的变化见图 11，可以看出焊缝位置对管材内外侧切向应变影响很小，但对周向应变及轴向应变有明显影响：当焊缝位于弯曲外侧和内侧时，焊缝区域周向应变显著增大，厚向应变有所减小；当焊缝位于弯曲外侧和中性层时，对弯曲

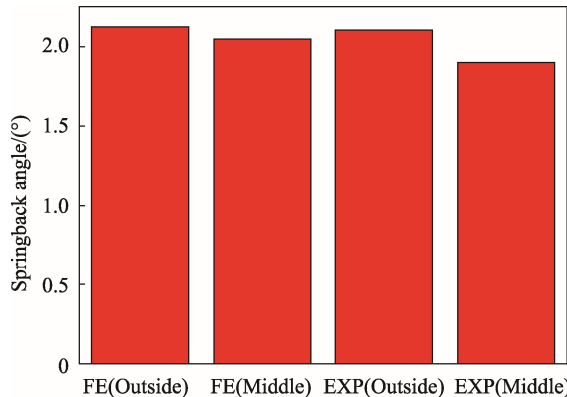


图 8 QSTE340 焊管数控弯曲模拟与实验回弹角结果对比<sup>[33]</sup>

Fig.8 Comparisons between simulated and experimental springback angle in QSTE340 welded tube bending

内侧应变影响很小,而当焊缝位于弯曲中性层和内侧时,对弯曲外侧应变分布影响很小。

图 12 所示为焊缝位于不同位置时对截面扁化及回弹的影响,从图 12a 可以看出,焊缝位于弯曲外侧和内侧时对截面扁化有较大影响,与均质管模型比较,截面扁化分别增大了 4.3% 和 1.7%;而焊缝位于中性层时,对截面扁化影响很小。这是由于焊缝位于内外侧时,其强材料属性增大了内外侧脊线的切向应力,

进而增大了内外侧管壁上切向应力在径向的合力,导致管材截面扁化增大。图 12b 显示,焊缝位于外侧、中性层和内侧时的回弹角相比于均质管模型的均增大了,但增大程度存在差异,3 种位置下回弹角分别增大 2.9%, 0.5%, 2.0%, 表明焊缝位于大变形区域时对回弹角的影响较大。

## 2.2 焊缝几何特征对管弯曲变形行为及变形协调规律影响

由 2.1 节分析可知,焊缝对管材弯曲过程中切向应变的影响较小,因此下面主要介绍焊缝对周向应变和厚向应变的影响。图 13 所示为焊缝宽度对焊管数控弯曲外侧应变的影响,其中焊缝宽度分别取 1.0(激光焊),2.8(高频电阻焊),5.0(闪光焊),10.0 mm(摩擦搅拌焊),焊缝和热影响区总宽度不变。从图 13 可以看出,随焊缝宽度增加,焊缝处周向应变逐渐增大,厚向应变逐渐减小;和均质管模型相比,周向应变分别增大 22.6%, 26.0%, 26.3%, 28.1%, 厚向应变分别减小 5.4%, 6.2%, 6.2%, 6.5%, 这些数据显示焊缝对周向应变和厚向应变的影响作用随焊缝宽度的增加而增大。综合来看焊缝约束作用的增大增强了焊缝对管材弯曲变形行为的影响。

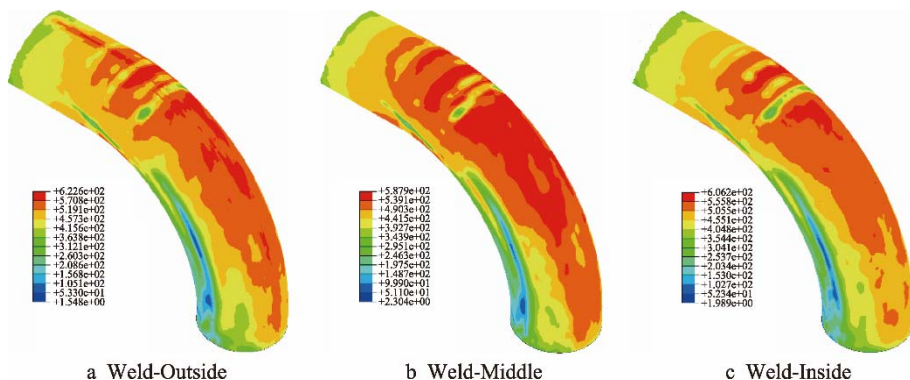


图 9 不同焊缝位置焊管数控弯曲等效应力 (MPa)<sup>[33]</sup>  
Fig.9 Equivalent stress distributions of welded tube in different weld positions

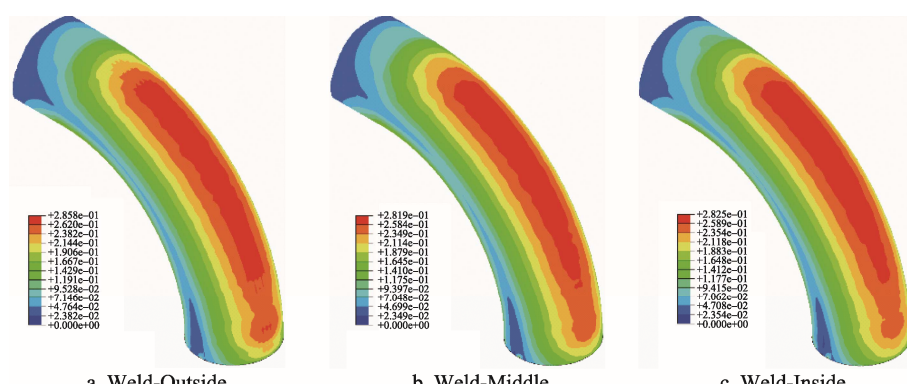


图 10 不同焊缝位置焊管数控弯曲等效应变分布<sup>[33]</sup>  
Fig.10 PEEQ distributions of welded tube in different weld positions

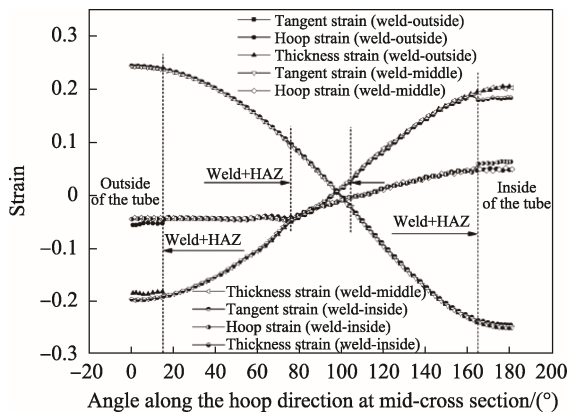


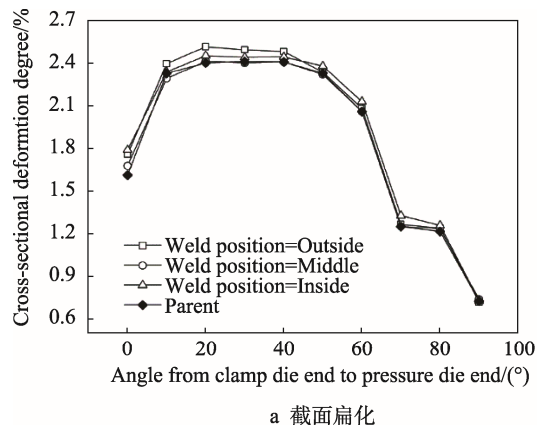
图 11 不同焊缝位置沿焊管弯曲平面中间截面应变变化<sup>[33]</sup>

Fig.11 Strain distributions along the mid-cross section of bending in different weld position

图 14 所示为焊缝宽度对焊管弯曲变形协调性的影响, 文献[33]定义焊缝、热影响区、母材区域界面处应变之比为变形协调比, 该变形协调比越接近均质管相同位置处的应变比, 说明协调性越好。从图 14 可以看出, 焊缝与热影响区三向应变的变形协调比  $W/H$  随着焊缝宽度的减小而逐渐趋近于均质管的比

值, 说明焊缝和热影响区的变形协调性随着焊缝宽度的减小而提高。这主要是由于热影响区性能分布不均匀, 其塑性变形能力沿周向越来越好, 随着焊缝宽度的减小, 靠近焊缝处热影响区的材料属性与焊缝的差异减小, 提高了焊缝和热影响区的变形协调性。而热影响区和母材三向应变的变形协调比  $H/P$  随焊缝宽度的增大变化很小, 这是由于焊缝宽度的变化并没有改变热影响区和母材接合处的材料属性, 且焊缝对热影响区变形的约束作用也很小, 从而对热影响区和母材接合处的变形影响较小。

图 15 所示为焊缝形状系数  $b_w/t$  对焊管数控弯曲外侧应变的影响, 其中管材壁厚分别取 1.0, 1.8, 2.7, 3.5 mm, 焊缝和热影响区的宽度不变, 相应的焊缝形状系数分别为 2.8, 1.6, 1.0, 0.8。从图 15 可以看出, 随  $b_w/t$  的增大, 管材外侧周向应变减小, 厚向应变逐渐增大; 与均质管模型相比, 焊缝处的周向应变分别增大了 25.6%, 26.0%, 59.2%, 148.7%, 厚向应变分别减小了 6.2%, 6.2%, 8.9%, 10.1%, 说明焊缝对周向应变和厚向应变的影响作用随  $b_w/t$  的增大而逐渐增大。这是由于随着  $b_w/t$  的增大, 管材实际壁厚减小, 厚向应变减弱, 而沿弯曲方向的变形量变化很小, 使圆周



a 截面扁化

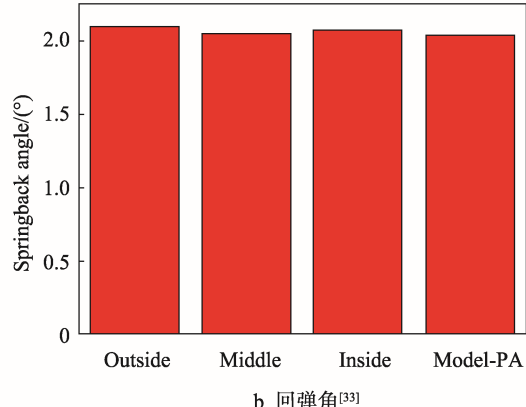
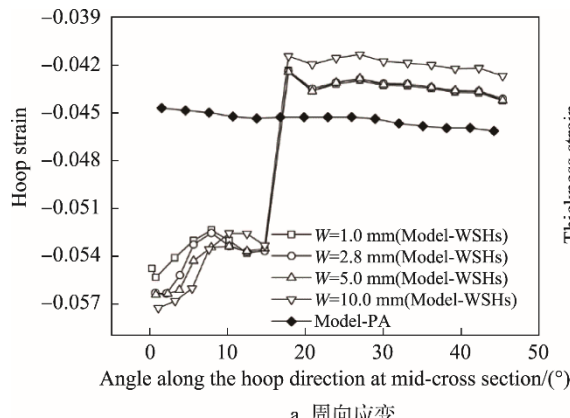
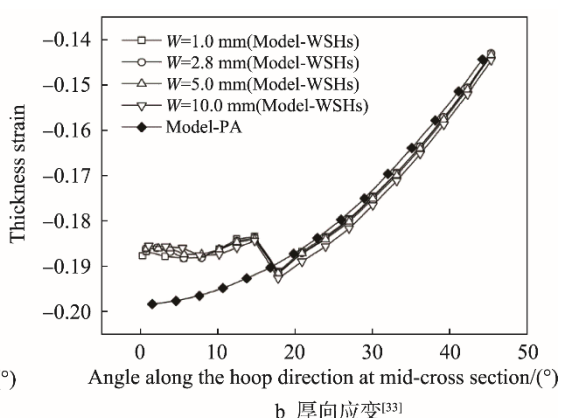


图 12 焊缝位置对截面扁化和回弹角的影响

Fig.12 Effects of weld position on cross-sectional deformation and springback angle



a 周向应变



b 厚向应变<sup>[33]</sup>

图 13 焊缝宽度对焊管弯曲外侧应变影响

Fig.13 Effects of weld width on the strain distributions along the outside of welded tube

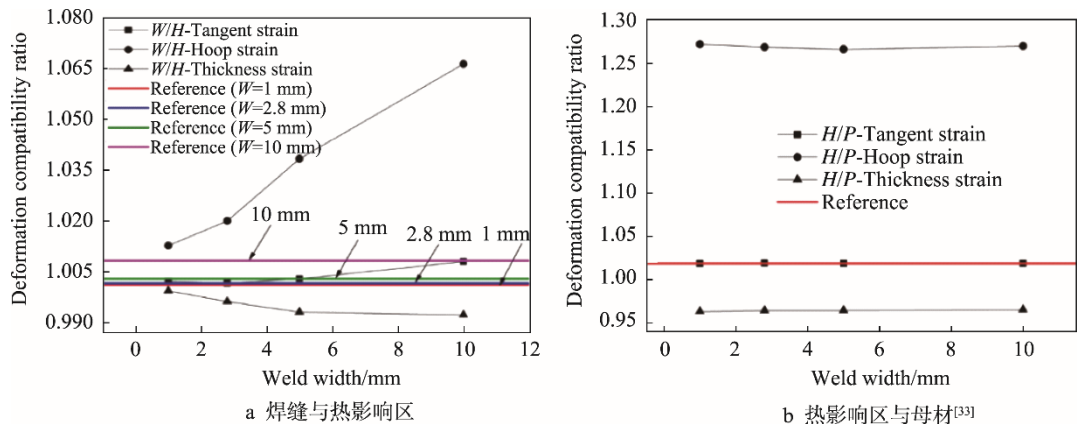


图 14 焊缝宽度对焊管弯曲变形协调影响  
Fig.14 Effects of weld width on deformation compatibility

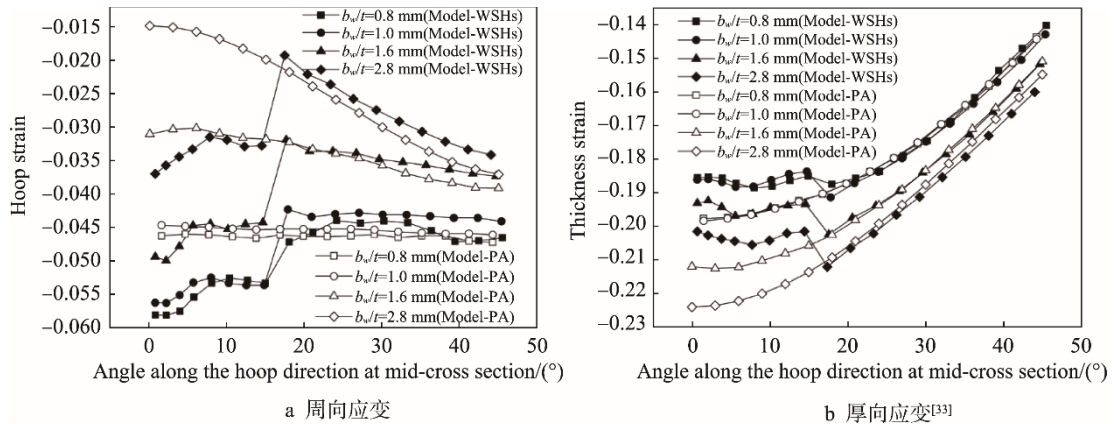


图 15 焊缝形状系数对焊管弯曲外侧应变影响  
Fig.15 Effects of weld-form factor on the strain distributions along the outside of welded tube

方向的金属流动量减小,这样就减小了管材弯曲外侧的周向应变,增大了厚向应变。相同变形条件下薄壁管先屈服,变形量较厚壁管大,所以焊缝对其约束作用较强。

图 16 所示为焊缝形状系数  $b_w/t$  对焊管弯曲变形协调性的影响,可以看出焊缝与热影响区厚向应变和周向应变的变形协调比  $W/H$  随着  $b_w/t$  的减小而逐渐趋近于均质管的比值,表明焊缝和热影响区的

变形协调性随  $b_w/t$  的减小而提高。同时热影响区和母材厚向应变及周向应变变形协调比  $H/P$  随  $b_w/t$  的变化规律与  $W/H$  的一致,即热影响区和母材的变形协调性也随着  $b_w/t$  的减小而提高。这是由于随着  $b_w/t$  的减小,管壁增厚,抵抗壁厚减薄的能力增强,且管材弯曲变形程度减小,导致不同组织区域应变差异减小,增强了焊管不同区域的变形协调性。

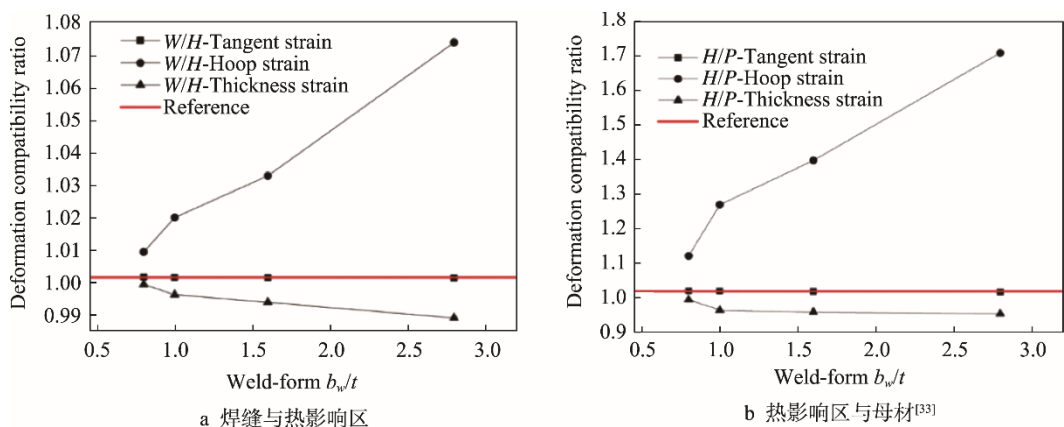


图 16  $b_w/t$  对焊管弯曲变形协调影响  
Fig.16 Effects of  $b_w/t$  on bending deformation compatibility of welding tube

### 2.3 焊管弯曲回弹预测

管材回弹预测中,解析模型凭借其能够快速、方便预测回弹而广泛应用,文献[36—41]建立了均质管回弹解析预测模型。焊管相比于均质管,其回弹影响因素更多,如2.1节分析显示,焊缝对回弹有影响,且影响程度依赖于焊缝位置,因此其回弹预测更加复杂。张必强<sup>[42]</sup>和Han等<sup>[43]</sup>建立了针对焊管回弹的解析预测模型,然而这两个模型内没有考虑焊缝不均匀力学属性及焊管几何特征,导致其预测误差较大。Zhan等<sup>[44]</sup>采用图17所示流程,依据静力平衡理论(见式(5)),考虑焊缝内不均匀力学属性连续变化特征及焊缝位置对回弹的影响,建立了焊管回弹解析预测模型(见式(6—8)),对比模型、文献预测结果及实验结果(见图18),验证了所得模型在焊管回弹预测中具有较高精度。

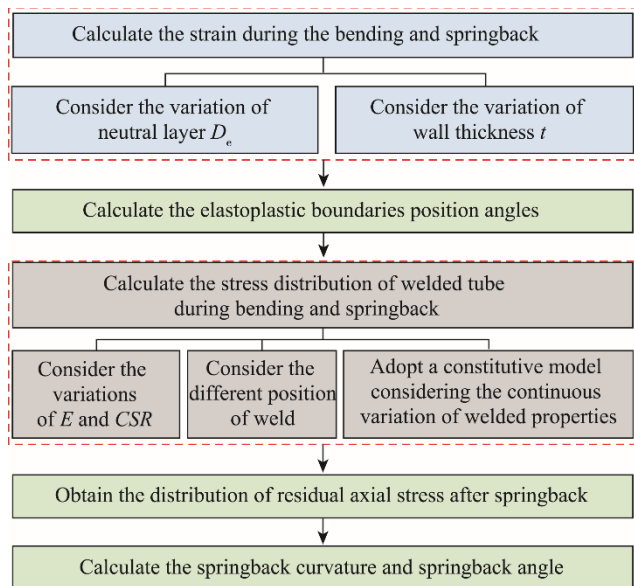


图17 考虑焊缝特征的焊管回弹解析模型建立流程<sup>[44]</sup>  
Fig.17 Flow chart of developing analytical springback model for welded tube bending

$$F_\theta = \int_0^A \sigma_\theta^r dA = 0 \quad (5)$$

式中: $F_\theta$ 是沿焊管截面的轴向合力; $\sigma_\theta^r$ 是回弹结束后沿焊管截面的残余轴向力; $A$ 是焊管截面积。

$$\Delta\theta = \frac{\rho_0 - D_e}{\rho_e + D_e} \theta \quad (6)$$

式中: $\Delta\theta$ 是回弹角; $\rho_0$ 是理论弯曲半径; $D_e$ 是中性层偏移量; $\theta$ 是弯曲角度; $\frac{1}{\rho_e + D_e}$ 依赖于焊缝位置。当焊缝位于弯曲内、外侧时,其由式(7)确定;当焊缝位于中性层时,其由式(8)确定。

$$\frac{1}{\rho_e + D_e} = \frac{C_{10} + C_{20} + C_{30} + C_{40} + C_{50}}{C_{w_0} + C_{H_0} + C_{p_0}},$$

$$\begin{aligned}
 C_{10} &= \int_0^{\varphi_{w_2}} Q(A\sigma_m^p + B\sigma_p^p) d\varphi \\
 C_{20} &= \int_{\varphi_{w_2}}^{\varphi_{H_2}} Q[\sigma_w^p - (\sigma_w^p - \sigma_p^p)(1 - e^{-\xi\varphi})] d\varphi \\
 C_{30} &= \int_{\varphi_{H_2}}^{\beta} Q\sigma_p^p d\varphi \\
 C_{40} &= \int_{\beta}^{\alpha} Q\sigma_p^e d\varphi \\
 C_{50} &= \int_{\alpha}^{\pi} -Q\sigma_p^p d\varphi \\
 C_{w_0} &= \int_0^{\varphi_{w_2}} \frac{E'_w Q}{1 - \nu_w^2} (y + D_e) d\varphi \\
 C_{H_0} &= \int_{\varphi_{w_2}}^{\varphi_{H_2}} \left[ \frac{E'_w}{1 - \nu_w^2} - \left( \frac{E'_w}{1 - \nu_w^2} - \frac{E'_p}{1 - \nu_p^2} \right) (1 - e^{-\xi\varphi}) \right] (y + D_e) Q d\varphi \\
 C_{p_0} &= \int_{\varphi_{H_2}}^{\pi} \frac{E'_p Q}{1 - \nu_p^2} (y + D_e) d\varphi \\
 \frac{1}{\rho_e + D_e} &= \frac{C_{11} + C_{21} + C_{31} + C_{41} + C_{51} + C_{61} + C_{71}}{C_{w_1} + C_{H_1} + C_{p_1}},
 \end{aligned} \tag{7}$$

$$\begin{aligned}
 C_{11} &= \int_{\varphi_{w_1}}^{\beta} Q(A\sigma_m^p + B\sigma_p^p) d\varphi \\
 C_{21} &= \int_{\beta}^{\alpha} Q\sigma_p^e d\varphi \\
 C_{31} &= \int_{\alpha}^{\varphi_{w_2}} -Q(A\sigma_m^p + B\sigma_p^p) d\varphi \\
 C_{41} &= \int_{\varphi_{H_1}}^{\varphi_{w_1}} Q[\sigma_w^p - (\sigma_w^p - \sigma_p^p)(1 - e^{-\xi\varphi})] d\varphi + \\
 &\quad \int_{\varphi_{w_2}}^{\varphi_{H_2}} Q[\sigma_w^p - (\sigma_w^p - \sigma_p^p)(1 - e^{-\xi\varphi})] d\varphi \\
 C_{51} &= \int_0^{\varphi_{H_1}} Q\sigma_p^p d\varphi + \int_{2\pi - \beta}^{2\pi} Q\sigma_p^p d\varphi \\
 C_{61} &= \int_{2\pi - \alpha}^{2\pi - \beta} Q\sigma_p^e d\varphi \\
 C_{71} &= \int_{\varphi_{H_2}}^{2\pi - \alpha} -Q\sigma_p^p d\varphi \\
 C_{w_1} &= \int_{\varphi_{w_1}}^{\varphi_{w_2}} \frac{E'_w Q}{1 - \nu_w^2} (y + D_e) d\varphi \\
 C_{H_1} &= \int_{\varphi_{H_1}}^{\varphi_{w_1}} \left[ \frac{E'_w}{1 - \nu_w^2} - \left( \frac{E'_w}{1 - \nu_w^2} - \frac{E'_p}{1 - \nu_p^2} \right) (1 - e^{-\xi\varphi}) \right] (y + D_e) Q d\varphi + \\
 &\quad \int_{\varphi_{w_2}}^{\varphi_{H_2}} \left[ \frac{E'_w}{1 - \nu_w^2} - \left( \frac{E'_w}{1 - \nu_w^2} - \frac{E'_p}{1 - \nu_p^2} \right) (1 - e^{-\xi\varphi}) \right] (y + D_e) Q d\varphi \\
 C_{p_1} &= \int_0^{\varphi_{H_1}} \frac{E'_p Q}{1 - \nu_p^2} (y + D_e) d\varphi + \int_{\varphi_{H_2}}^{2\pi} \frac{E'_p Q}{1 - \nu_p^2} (y + D_e) d\varphi
 \end{aligned} \tag{8}$$

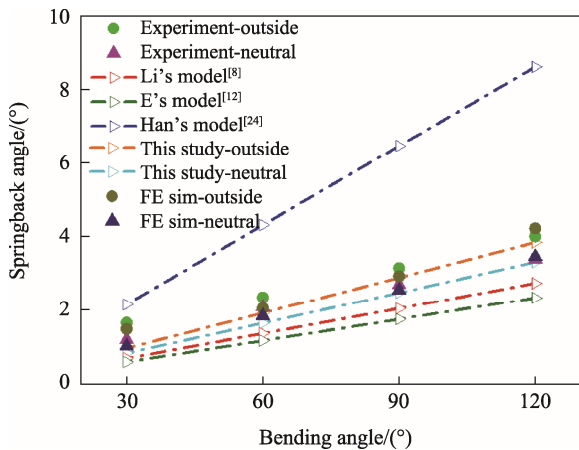
图 18 不同解析模型预测得的回弹角及实验结果对比<sup>[44]</sup>

Fig.18 Experimental and predicted springback angles by different models

### 3 拼焊板旋压成形

拼焊板旋压在航空航天领域燃料储箱封头类大型薄壁异型曲面构件(见图 19)的制备中,凭借其能够实现该类构件高效成形而成为重要技术路线,西北工业大学詹梅教授团队在该类型拼焊板构件旋压有限元建模及工艺设计方面取得了进展<sup>[45]</sup>。

有限元建模方面,根据构件形状特征和旋压变形特征,确定了旋轮运动轨迹(见式(9)和见图 20),解决了接触、网格等关键建模技术,建立了 2219 铝合金拼焊板旋压有限元模型(见图 21)。通过对比模拟与实验相同条件下试件外轮廓图验证了模型可靠性(见图 22)。

$$\left\{ \begin{array}{l} x_{P_1} = x_{B_i} + \rho \frac{x_{B_i}}{R} + (D_R / 2 - \rho) \cos \beta - (t_R - \rho) \sin \beta \\ y_{P_1} = y_{B_i} + \rho \frac{y_{B_i} - y_{o'}}{R} + (D_R / 2 - \rho) \sin \beta + (t_R - \rho) \cos \beta \\ x_{P_2} = x_{B_i} + b^2 x_{A_i} \rho / \sqrt{a^4 y_{A_i}^2 + b^4 x_{A_i}^2} + (D_R / 2 - \rho) \cos \beta - (t_R - \rho) \sin \beta \\ y_{P_2} = y_{B_i} + b^2 x_{A_i} \rho / \sqrt{a^4 y_{A_i}^2 + b^4 x_{A_i}^2} + (D_R / 2 - \rho) \sin \beta + (t_R - \rho) \cos \beta \end{array} \right. \quad (9)$$

式中:  $(x_{P_1}, y_{P_1})$ ,  $(x_{P_2}, y_{P_2})$  分别是锥段与椭球段旋轮参考点坐标;  $\rho$  为旋轮圆角半径;  $R$  为锥段半径;

$t_R$  为旋轮厚度;  $D_R$  为旋轮直径;  $\beta$  为旋轮安装角度;  $(x_{Bi}, y_{Bi})$  为旋轮与构件外表面相切点坐标。

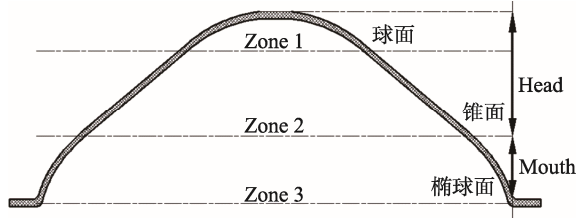


图 19 燃料储箱封头类大型薄壁异型曲面构件示意图  
Fig.19 Schematic of large thin-walled special-shaped curved components for fuel tank head

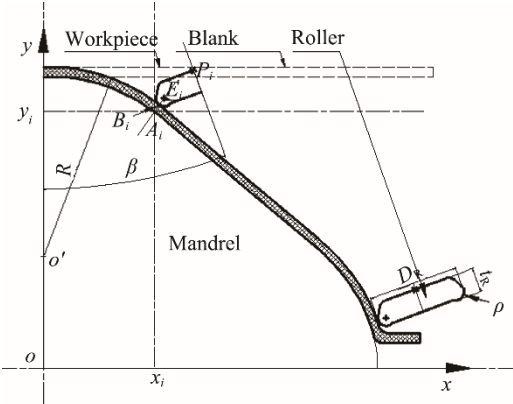


图 20 拼焊板旋压成形薄壁异型曲面构件旋轮运动轨迹示意图<sup>[45]</sup>  
Fig.20 Schematic of roller moving trail in spinning thin-walled special-shaped curved head components

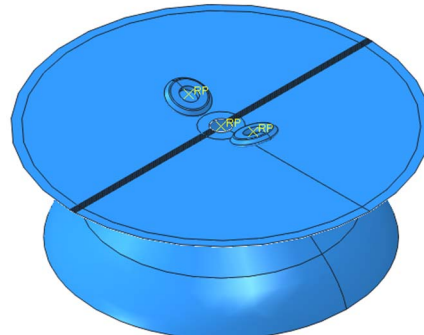


图 21 2219 铝合金拼焊板旋压成形薄壁异型曲面构件有限元模型<sup>[45]</sup>  
Fig.21 Finite element model for spinning thin-walled special-shaped curved head components by 2219 aluminum alloy tailor welded plate



a 试验件

b 模拟件<sup>[45]</sup>

图 22 2219 铝合金拼焊板旋压成形薄壁异型曲面构件模拟和试验件

Fig.22 Simulation and test pieces for spinning formed thin-walled special-shaped curved head components by 2219 aluminum alloy tailor welded plate

工艺设计方面,开展了2219铝合金拼焊板旋压成形大型薄壁异型曲面构件1/5缩比件试验研究。针对收口过程变形量大,成形特征接近筒形件拉深旋压,加之口部壁厚薄、直径大,采用一道次贴模成形很容易出现凸缘起皱的问题,确定了如图23所示的五道次强旋-普旋结合成形方案。采用上述方案最终成功旋制出拼焊板薄壁异型曲面构件(见图24)。

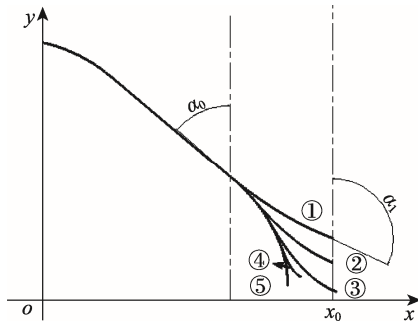


图23 拼焊板旋压成形薄壁异型曲面构件渐进贴模成形轨迹<sup>[45]</sup>

Fig.23 Progressive forming trajectory in the spinning of thin-walled special-shaped curved head components of tailor welded plate



图24 拼焊板薄壁异型曲面旋压成形件<sup>[45]</sup>

Fig.24 Final thin-walled special-shaped curved head spun component of tailor welded plate

## 4 结论

轻量化拼焊板构件塑性成形是飞机、汽车工业中的关键技术,具有广阔应用前景,但由于焊缝引入的材料、几何、边界条件非线性显著增加了成形复杂性,导致成形质量及成形极限下降。目前,国内外学者在拼焊板构件材料不均匀力学行为表征、塑性成形变形机理及成形规律等方面取得了一定进展,为发展轻量化拼焊板构件塑性成形提供了指导,但仍面临以下困难和挑战:①如何揭示拼焊板构件塑性成形中的不均匀变形协调机理;②拼焊板构件塑性成形稳定性和缺陷敏感性与不均匀变形间的映射关系;③考虑拼焊板构件微观组织差异的损伤断裂预测模型建立;④如何实现拼焊板构件损伤演化与成形质量一体化调控,提高拼焊板构件塑性成形极限。

## 参考文献:

- [1] KOC M, ALTAN T. An Overall Review of the Tube Hydroforming (THF) Technology[J]. Journal of Materials Processing Technology, 2001, 108: 384—393.
- [2] AHMETOGLU M, ALTAN T. Tube Hydroforming: State-of-the-art and Future Trends[J]. Journal of Materials Processing Technology, 2000, 98: 25—33.
- [3] YANG J B, JEON B H, OHS I. The Tube Bending Technology of a Hydroforming Process for an Automotive Part[J]. Journal of Materials Processing Technology, 2001, 111: 175—181.
- [4] TRANA K. Finite Element Simulation of the Tube Hydroforming Process-bending, Preforming and Hydroforming[J]. Journal of Materials Processing Technology, 2002, 127: 401—408.
- [5] ZHAN M, GUO K, YANG H. Advances and Trends in Plastic Forming Technologies for Welded Tubes[J]. Chinese Journal of Aeronautics, 2016, 29: 305—315.
- [6] LIU G, CHU G N, YUAN S J. Deformation Evolution Mechanism during Hydro-bulging of Tailor-welded Tube with Dissimilar Thickness[J]. International Journal of Advanced Manufacturing Technology, 2010, 46: 111—116.
- [7] LIU G, YUAN S J, CHU G N. FEA on Deformation Behavior of Tailor-welded Tube in Hydroforming[J]. Journal of Materials Processing Technology, 2007, 187/188: 287—291.
- [8] 初冠南, 刘钢, 苑世剑. 差厚拼焊管内高压胀形塑性变形规律[J]. 金属学报, 2008, 44: 1479—1484.  
CHU Guan-nan, LIU Gang, YUAN Shi-jian. Plastic Deformation Regularity of Tailor-welded Tube (TWT) with Dissimilar Thickness during Hydro-bulging[J]. Acta Metallurgica Sinica, 2008, 44: 1479—1484.
- [9] CHU G N, LIU G, LIU W J. An Approach to Improve Thickness Uniformity within Tailor-welded Tube Hydroforming[J]. International Journal of Advanced Manufacturing Technology, 2012, 60: 1247—1253.
- [10] 张立玲, 高峰, 杜发荣. 不等厚拼焊管轴向压缩变形的数值模拟研究[J]. 塑性工程学报, 2006, 13(4): 6—9.  
ZHANG Li-ling, GAO Feng, DU Fa-rong. Numerical Simulation Study on Axial Compression Deformation of Unequal Thick Welded Tubes[J]. Journal of Plasticity Engineering, 2006, 13(4): 6—9.
- [11] 陈锡荣, 林忠钦, 李淑慧, 等. 基于数值模拟的拼焊板焊缝移动控制方法研究[J]. 汽车技术, 2004(2): 30—33.  
CHEN Xi-rong, LIN Zhong-qin, LI Shu-hui, et al. Study on the Numerical Simulation Based Control Method for Movement of Welding Beam of Welding Splice Piecess[J]. Automobile Technology, 2004(2): 30—33.
- [12] HEO Y M, CHOI Y, KIM H Y. Characteristics of Weld Line Movements for Deep Drawing with Drawbeads of

- Tailor-welded Blanks[J]. *Journal of Materials Processing Technology*, 2001, 111: 164—169.
- [13] CHAN S M, CHAN L C, LEE T C. Tailor-welded Blanks of Different Thickness Ratios Effects on Forming Limit Diagrams[J]. *Journal of Materials Processing Technology*, 2003, 132: 95—101.
- [14] HEO Y M, WANG S H, KIM H Y, et al. The Effect of Drawbead Dimensions on the Weld-line Movements in the Deep Drawing of Tailor-welded Blanks[J]. *Journal of Materials Processing Technology*, 2001, 113: 686—691.
- [15] TANGB T, ZHAO Z, YU S, et al. One-step FEM Based Control of Weld Line Movement for Tailor-weld Blanks Forming[J]. *Journal of Materials Processing Technology*, 2007, 187/188: 383—386.
- [16] QIU X G, CHEN W L. The Study on Numerical Simulation of the Laser Tailor Welded Blanks Stamping[J]. *Journal of Materials Processing Technology*, 2007, 187/188: 128—131.
- [17] 张福祥, 陈炜, 杨继昌, 等. 拼焊板在盒形件拉伸过程中的焊缝移动研究[J]. 精密成形工程, 2002(5): 33—36.  
ZHANG Fu-xiang, CHENG Wei, YANG Ji-chang, et al. Research on Welding Line Movement for TWB during Square Cup Drawing[J]. *Journal of Netshape Forming Engineering*, 2002(5): 33—36.
- [18] 陈炜, 杨继昌, 林忠钦. 拼焊板覆盖件成形过程中的焊缝移动和成形性能[J]. 机械工程学报, 2004, 40(9): 62—66.  
CHENG Wei, YANG Ji-chang, LIN Zhong-qin. Weld Movement and Forming Properties during the Forming of Tailor Welded Blanks[J]. *Chinese Journal of Mechanical Engineering*, 2004, 40(9): 62—66.
- [19] GHOOB Y, KEUM Y T, KIM Y S. Evaluation of the Mechanical Properties of Welded Metal in Tailored Steel Sheet Welded by CO<sub>2</sub> Laser[J]. *Journal of Materials Processing Technology*, 2001, 113: 692—698.
- [20] PANDA S K, KUMAR D R, KUMA R H, et al. Characterization of Tensile Properties of Tailor Welded IF Steel Sheets and Their Formability in Stretch Forming[J]. *Journal of Materials Processing Technology*, 2007, 183: 321—332.
- [21] ZADPOOR A A, SINKE J, BENEDICTUS R, et al. Mechanical Properties and Microstructure of Friction Stir Welded Tailor-made Blanks[J]. *Materials Science & Engineering A*, 2008, 494: 281—290.
- [22] CHENG C H, JIE M, CHAN L C, et al. True Stress-strain Analysis on Weldment of Heterogeneous Tailor-welded Blanks-a Novel Approach for Forming Simulation[J]. *International Journal of Mechanical Sciences*, 2007, 49: 217—229.
- [23] LEE W, CHUNG K H, KIM D, et al. Experimental and Numerical Study on Formability of Friction Stir Welded TWB Sheets Based on Hemispherical Dome Stretch Tests[J]. *International Journal of Plasticity*, 2009, 25: 1626—1654.
- [24] REI S A, TEIXEIR A P, DUARTE J F, et al. Tailored Welded Blanks-an Experimental and Numerical Study in Sheet Metal Forming on the Effect of Welding[J]. *Computers & Structures*, 2004, 82: 1435—1442.
- [25] LI G, XU F, SUN G, et al. Identification of Mechanical Properties of the Weld Line by Combining 3D Digital Image Correlation with Inverse Modeling Procedure[J]. *International Journal of Advanced Manufacturing Technology*, 2014, 74: 893—905.
- [26] SONG Y L, HUA L, MENG F Z. Inhomogeneous Constructive Modelling of Laser Welded Bead Based on Nanoindentation Test[J]. *IronmakSteelmak*, 2012, 39: 95—103.
- [27] ZHAN M, DU H, LIU J, et al. A Method for Establishing the Plastic Constitutive Relationship of the Weld Bead and Heat-affected Zone of Welded Tubes Based on the Rule of Mixtures and a Microhardnesstest[J]. *Materials Science & Engineering A*, 2010, 527: 2864—2874.
- [28] XING L, ZHAN M, GAO P F, et al. A Method for Establishing a Continuous Constitutive Model of Welded Metals[J]. *Materials Science & Engineering A*, 2018, 718: 228—240.
- [29] REN N, ZHAN M, YANG H, et al. Constraining Effects of Weld and Heat-affected Zone on Deformation Behaviors of Welded Tubes in Numerical Control Bending Process[J]. *Journal of Materials Processing Technology*, 2012, 212: 1106—1115.
- [30] REN N, YANG H, ZHAN M, et al. Strain Distribution Characteristics of Welded Tube in NC Bending Process Using Experimental Grid Method[J]. *International Journal of Advanced Manufacturing Technology*, 2013, 66: 635—644.
- [31] REN N, YANG H, ZHAN M, et al. Effect of Weld Characteristics on the Formability of Welded Tubes in NC Bending Process[J]. *International Journal of Advanced Manufacturing Technology*, 2013, 69: 181—195.
- [32] YANG H, REN N, ZHAN M, et al. Experimental and Numerical Studies on the Prediction of Bendability Limit of QSTE340 Welded Tube in NC Bending Process[J]. *Science China Technological Sciences*, 2012, 55: 2264—2277.
- [33] 任宁. 钢钢管数控弯曲变形协调规律及成形极限研究[D]. 西安: 西北工业大学, 2013.  
REN Ning. Study on Deformation Compatibility and Bending Limit in Steel Welded Tube NC Bending Processes[D]. Xi'an: Northwestern Polytechnical University, 2013.
- [34] REN N, ZHAN M, YANG H, et al. Weld Characteristic and NC Bending Formability Study of QSTE340 Welded Tube[J]. *Transactions of Tianjin University*, 2011, 17:

288—292.

- [35] REN N, ZHAN M, YANG H, et al. Significance Analysis of Weld and Processing Parameters on Wall Thinning and Cross-sectional Deformation of Welded Tube in NC Bending Process[J]. Advances in Heterogeneous Material Mechanics, 2011: 457—460.
- [36] LI H, YANG H, SONG F F, et al. Springback Characterization and Behaviors of High-strength Ti-3Al-2.5V Tube in Cold Rotary Draw Bending[J]. Journal of Materials Processing Technology, 2012, 212: 1973—1987.
- [37] ZHAO J, ZHAI R X, MA R, et al. Springback Theory of Plane Bending and the Progress of Study on Its Engineering Application[J]. Steel Research International, 2013, 84: 1230—1240.
- [38] ZHANG Z K, WU J J, GUO R C, et al. A Semi-analytical Method for the Springback Prediction of Thick-walled 3D Tubes[J]. Materials Design, 2016, 99: 57—67.
- [39] ZHAN M, YANG H, HUANG L, et al. Springback Analysis of Numerical Control Bending of Thin-walled Tube Using Numerical-analytic Method[J]. Journal of Materials Processing Technology, 2006, 177: 197—201.
- [40] E D X, HE H H, LIU X Y, et al. Spring-back Deformation in Tube Bending[J]. International Journal of Minerals Metallurgy and Materials, 2009, 16: 177—183.
- [41] ZHAN M, WANG Y, YANG H, et al. An Analytic Model for Tube Bending Springback Considering Different Parameter Variations of Ti-alloy Tubes[J]. Journal of Materials Processing Technology, 2016, 236: 123—137.
- [42] 张必强. 焊管成形时的回弹[J]. 上海钢研, 1994(3): 28—31.
- ZHANG Bi-qiang. The Springback in Forming of Welding Tube and Pipe[J]. Shanghai Steel Iron Research, 1994(3): 28—31.
- [43] HAN C, FENG H, YUAN S J. Springback and Compensation of Bending for Hydroforming of Advanced High-strength Steel Welded Tubes[J]. International Journal of Advanced Manufacturing Technology, 2017, 89: 3619—3629.
- [44] ZHAN M, XING L, GAO P F, et al. An Analytical Springback Model for Bending of Welded Tube Considering the Weld Characteristics[J]. International Journal of Mechanical Sciences, 2019, 150: 594—609.
- [45] 雷新鹏. 2219 铝合金拼焊板旋压成形异型曲面规律与工艺设计研究[D]. 西安: 西北工业大学, 2018.
- LEI Xin-peng. Research on Deformation Rules and Processing Design for the Spinning of Profiled Surface Component with Welded-blank[D]. Xi'an: Northwestern Polytechnical University, 2018.